Applied Mathematical Modelling 39 (2015) 6258–6272

Contents lists available at ScienceDirect

Applied Mathematical Modelling

journal homepage: www.elsevier.com/locate/apm

An inverse time-dependent source problem for the heat equation with a non-classical boundary condition

A. Hazanee [a], D. Lesnic [a,*], M.I. Ismailov [b], N.B. Kerimov [c]

[a] Department of Applied Mathematics, University of Leeds, Leeds LS2 9JT, UK
[b] Department of Mathematics, Gebze Institute of Technology, Gebze, Kocaeli 41400, Turkey
[c] Department of Mathematics, Mersin University, Mersin 33343, Turkey

ARTICLE INFO

Article history:
Received 7 January 2014
Received in revised form 22 December 2014
Accepted 19 January 2015
Available online 7 February 2015

Keywords:
Heat equation
Inverse source problem
Non-classical boundary conditions
Generalised Fourier method

ABSTRACT

This paper investigates the inverse problem of determining the time-dependent heat source and the temperature for the heat equation with a non-classical boundary and an integral over-determination conditions. The existence, uniqueness and continuous dependence upon the data of the classical solution of the inverse problem is shown by using the generalised Fourier method. Furthermore in the numerical process, the boundary element method (BEM) together with the second-order Tikhonov regularization is employed with the choice of regularization parameter based on the generalised cross-validation (GCV) criterion. Numerical results are presented and discussed.

1. Introduction

Inverse time-dependent source problems for the heat equation with local, nonlocal, integral or nonclassical (boundary) conditions have become the point of interest in many recent papers, [1–7], to name only a few. In the present paper, we consider yet another reconstruction of a time-dependent heat source from an integral over-determination measurement of the thermal energy of the system and a new dynamic-type boundary condition.

Let $T > 0$ be a fixed number and denote by $D_T = \{(x,t) : 0 < x < 1, 0 < t \leqslant T\} = (0,1) \times (0,T]$. Consider the following initial-boundary value problem for the heat equation:

$$u_t = u_{xx} + r(t)f(x,t), \quad (x,t) \in \overline{D}_T, \tag{1.1}$$

$$u(x,0) = \varphi(x), \quad x \in (0,1), \tag{1.2}$$

$$u(0,t) = 0, \quad t \in (0,T], \tag{1.3}$$

$$au_{xx}(1,t) + du_x(1,t) + bu(1,t) = 0, \quad t \in (0,T], \tag{1.4}$$

where f, φ are given functions and a, b, d are given numbers not simultaneously equal to zero. When the function $r(t)$ is given, the problem of finding $u(x,t)$ from the heat Eq. (1.1), initial condition (1.2), and boundary conditions (1.3) and (1.4) is termed as the direct (or forward) problem. The well-posedness of this direct problem has been established elsewhere, [8].

* Corresponding author.
E-mail addresses: mmah@leeds.ac.uk (A. Hazanee), amt5ld@maths.leeds.ac.uk (D. Lesnic), mismailov@gyte.edu.tr (M.I. Ismailov), nazimkerimov@yahoo.com (N.B. Kerimov).

http://dx.doi.org/10.1016/j.apm.2015.01.058
0307-904X/

This model can be used in heat transfer and diffusion processes with a source parameter present in (1.1). Also, in acoustic scattering or damage corrosion the dynamic boundary condition (1.4) is also known as a generalised impedance boundary condition, [9–12].

Taking into account the Eq. (1.1) at $x = 1$, the boundary condition (1.4) becomes

$$au_t(1,t) + du_x(1,t) + bu(1,t) = ar(t)f(1,t), \quad t \in (0,T]. \tag{1.5}$$

In order to add further physics to the problem, we mention that the boundary condition (1.5) is observed in the process of cooling of a thin solid bar one end of which is placed in contact with a fluid [13]. Another possible application of such type of boundary condition is announced in [14, p. 79], as this boundary condition represents a boundary reaction in diffusion of chemical. We finally mention that we have also previously encountered the dynamic boundary condition (1.5) when modelling a transient flow pump experiment in a porous medium [15].

When the function $r(t)$ for $t \in [0,T]$ is unknown, the inverse problem formulates as that of finding a pair of functions $(r(t), u(x,t))$ which satisfy the Eq. (1.1), initial condition (1.2), the boundary conditions (1.3) and (1.4) (or (1.5)), and the energy/mass overdetermination measurement

$$\int_0^1 u(x,t)\,dx = E(t), \quad t \in [0,T]. \tag{1.6}$$

It is also worth mentioning that a related parabolic inverse source problem given by equations (1.1)–(1.3), (1.6) and the following dynamic boundary condition

$$u_t(1,t) + u_x(1,t) + \sigma(u(1,t)) = 0, \quad t \in (0,T], \tag{1.7}$$

where σ is a given Lipschitz function, has very recently been investigated in [16]. However, no numerical results were presented and the boundary condition (1.7) is different of the boundary condition (1.5) considered in the present study.

The condition (1.6) is encountered in modelling applications related to particle diffusion in turbulent plasma, as well as in heat conduction problems in which the law of variation $E(t)$ of the total energy of heat in a rod is given, [17].

If we let $u(x,t)$ represent the temperature distribution, then the above-mentioned inverse problem can be regarded as a source control problem. The source control parameter $r(t)$ needs to be determined from the measurement of the thermal energy $E(t)$.

Because the function r is space independent, a, b and d are constants and the boundary conditions are linear and homogeneous, the method of separation of variables is suitable for studying the problem under consideration. It is well-known that the main difficulty in applying the Fourier method is the explicit availability of a basis, i.e. the expansion in terms of eigenfunctions of the auxiliary spectral problem

$$\begin{cases} y''(x) + \mu y(x) = 0, \quad x \in [0,1], \\ y(0) = 0, \\ (a\mu - b)y(1) = dy'(1). \end{cases} \tag{1.8}$$

In contrast to the classical Sturm–Liouville problem, this problem has the spectral parameter also in the boundary condition. It makes it impossible to apply the classical results on expansion in terms of eigenfunctions [18]. The spectral analysis of such type of problems was started by [19]. After that, important developments were made by [20–24]. It is useful to note the reference [25] whose results on expansion in term of eigenfunctions will be used in the present paper.

The paper is organised as follows. In Section 2, the eigenvalues and eigenfunctions of the auxiliary spectral problem and some of their properties are introduced. Then the existence, uniqueness, and continuous dependence upon the data of the solution of the inverse problem (1.1)–(1.3), (1.5), (1.6) are proved. The numerical discretisation of the inverse problem is based on the boundary element method (BEM) which is described in Section 3. Section 4 discusses numerical results obtained for a couple of benchmark test examples and emphasises the importance of employing regularization in order to achieve a stable numerical solution. Finally, Section 5 presents the conclusions of the paper.

2. Mathematical analysis

Consider the spectral problem (1.8) with $ad > 0$. It is known from [20] that its eigenvalues $\mu_n, n = 0,1,2,\ldots$ are real and simple. They form an unbounded increasing sequence and the eigenfunction $y_n(x)$ corresponding to μ_n has exactly n simple zeros in the interval $(0,1)$. We can also give the sign of the first eigenvalue μ_0 as

$$\begin{cases} \mu_0 < 0 < \mu_1 < \mu_2 < \cdots, \text{if } -\frac{b}{d} > 1, \\ \mu_0 = 0 < \mu_1 < \mu_2 < \cdots, \text{if } -\frac{b}{d} = 1, \\ 0 < \mu_0 < \mu_1 < \mu_2 < \cdots, \text{if } -\frac{b}{d} < 1. \end{cases}$$

It was shown in [25] that the eigenvalues and eigenfunctions have the following asymptotic behaviour:

$$\sqrt{\mu_n} = \pi n + O\left(\frac{1}{n}\right), \quad y_n(x) = \sin(\pi n x) + O\left(\frac{1}{n}\right),$$

for sufficiently large n.

Let n_0 be arbitrary fixed non-negative integer. It was shown in [25] that the system of eigenfunctions $\{y_n(x)\}$ $(n = 0, 1, 2, \ldots; n \neq n_0)$ is a Riesz basis for $L_2[0,1]$. The system $\{u_n(x)\}$ $(n = 0, 1, 2, \ldots; n \neq n_0)$ which is biorthogonal to the system $\{y_n(x)\}$ $(n = 0, 1, 2, \ldots; n \neq n_0)$ has the form

$$u_n(x) = \frac{y_n(x) - \frac{y_n(1)}{y_{n_0}(1)} y_{n_0}(x)}{\|y_n\|^2_{L_2[0,1]} + \frac{a}{d} y_n^2(1)}.$$

The following Bessel-type inequalities are true for the systems $\{y_n(x)\}$ and $\{u_n(x)\}$ $(n = 0, 1, 2, \ldots; n \neq n_0)$, see [8].

Lemma 1 (Bessel-type inequalities). *If $\psi(x) \in L_2[0,1]$, then the estimates*

$$\sum_{\substack{n=0 \\ (n \neq n_0)}}^{\infty} |(\psi, y_n)|^2 \leqslant c_1 \|\psi\|^2_{L_2[0,1]}, \quad \sum_{\substack{n=0 \\ (n \neq n_0)}}^{\infty} |(\psi, u_n)|^2 \leqslant c_2 \|\psi\|^2_{L_2[0,1]}$$

hold for some positive constants c_1 and c_2, where $(\psi, y_n) = \int_0^1 \psi(x) y_n(x) dx$ and $(\psi, u_n) = \int_0^1 \psi(x) u_n(x)\, dx$ denote the usual inner products in $L_2[0,1]$.

Let us denote $\Phi^4_{n_0}[0,1] := \{\psi(x) \in C^4[0,1]; \psi(0) = \psi''(0) = 0, \psi(1) = \psi'(1) = \psi''(1) = \psi'''(1) = 0, \int_0^1 \psi(x) y_{n_0}(x) dx = 0\}$.

Lemma 2. *If $\psi(x) \in \Phi^4_{n_0}[0,1]$, then we have:*

$$\mu_n^2(\psi, y_n) = (\psi^{(4)}, y_n), \quad \mu_n^2(\psi, u_n) = (\psi^{(4)}, u_n), \quad n \geqslant 0, \tag{2.1}$$

$$\sum_{\substack{n=0 \\ (n \neq n_0)}}^{\infty} |\mu_n(\psi, y_n)| \leqslant c_3 \|\psi\|_{C^4[0,1]}, \quad \sum_{\substack{n=0 \\ (n \neq n_0)}}^{\infty} |\mu_n(\psi, u_n)| \leqslant c_4 \|\psi\|_{C^4[0,1]}, \tag{2.2}$$

$$\sum_{\substack{n=0 \\ (n \neq n_0)}}^{\infty} |(\psi, y_n)| \leqslant c_5 \|\psi\|_{C^4[0,1]}, \quad \sum_{\substack{n=0 \\ (n \neq n_0)}}^{\infty} |(\psi, u_n)| \leqslant c_6 \|\psi\|_{C^4[0,1]}, \tag{2.3}$$

where c_3, c_4, c_5 and c_6 are some positive constants.

Proof. From (1.8), since $\mu_n y_n = -y_n''$ and $y_n(0) = 0$, the identities (2.1) follow by applying four times integration by parts in (1.8) and using that $\psi \in \Phi^4_{n_0}[0,1]$. The estimates (2.2) are obtained from Lemma 1, Eq. (2.1) and using the Schwarz inequality. Finally, since for a sufficiently large m the series $\sum_{n=m}^{\infty} |\mu_n(\psi, y_n)|$ is majorant for the series $\sum_{n=m}^{\infty} |(\psi, y_n)|$, the estimates (2.3) also hold. □

Theorem 1 (*Existence and uniqueness*). *Let the following conditions be satisfied:*

- (A_1) $\varphi(x) \in \Phi^4_{n_0}[0,1]$.
- (A_2) $E(t) \in C^1[0,T]; E(0) = \int_0^1 \varphi(x) dx$.
- (A_3) $f(x,t) \in C(\overline{D}_T)$; $f(x,t) \in \Phi^4_{n_0}[0,1], \forall t \in [0,T]$; $\int_0^1 f(x,t) dx \neq 0, \forall t \in [0,T]$.

Then the inverse problem (1.1)–(1.3), (1.5), (1.6) has a unique classical solution $(r(t), u(x,t)) \in C[0,T] \times (C^{2,1}(D_T) \cap C^{2,0}(\overline{D}_T))$. Moreover, $u(x,t) \in C^{2,1}(\overline{D}_T)$.

Proof. For given $r(t) \in C[0,T]$, to construct the formal solution $u(x,t)$ of the direct problem (1.1)–(1.3), (1.5) we will use the generalised Fourier method. Based on this method, the solution $u(x,t)$ is sought in a Fourier series in terms of the eigenfunctions $\{y_n(x)\}$ $(n = 0, 1, 2, \ldots; n \neq n_0)$ of the auxiliary spectral problem (1.8), namely,

$$u(x,t) = \sum_{\substack{n=0 \\ (n \neq n_0)}}^{\infty} v_n(t) y_n(x), \quad v_n(t) = (u, u_n).$$

The functions $v_n(t), n = 0, 1, 2, \ldots; n \neq n_0$, satisfy the Cauchy problem

$$\begin{cases} v_n'(t) + \mu_n v_n(t) = r(t) f_n(t), \\ v_n(0) = \varphi_n, \end{cases}$$

where $f_n(t) = (f, u_n)$ and $\varphi_n = (\varphi, u_n)$. Solving these Cauchy problems, we obtain

$$v_n(t) = \varphi_n e^{-\mu_n t} + \int_0^t r(\tau) f_n(\tau) e^{-\mu_n (t-\tau)} d\tau,$$

and then formally,

$$u(x,t) = \sum_{\substack{n=0 \\ (n \neq n_0)}}^{\infty} \left[\varphi_n e^{-\mu_n t} + \int_0^t r(\tau) f_n(\tau) e^{-\mu_n (t-\tau)} d\tau \right] y_n(x). \tag{2.4}$$

Under the conditions (A_1) and (A_3), the series (2.4) and its x-partial derivative are uniformly convergent in $\overline{D}_T$ since their majorizing sums are absolutely convergent, see the inequalities (2.2) and (2.3). Therefore, their sums $u(x,t)$ and $u_x(x,t)$ are continuous in $\overline{D}_T$. The t-partial derivative and the xx-second-order partial derivative series also are uniformly convergent in $\overline{D}_T$. Thus, $u(x,t) \in C^{2,1}(\overline{D}_T)$ and satisfies the conditions (1.1)–(1.3), (1.5) for arbitrary $r(t) \in C[0,T]$.

The formulas (2.4) and (1.6) yield a following Volterra integral equation of the first kind with respect to $r(t)$:

$$\int_0^t K(t,\tau) r(\tau) d\tau + F(t) = E(t), \tag{2.5}$$

where

$$F(t) = \sum_{\substack{n=0 \\ (n \neq n_0)}}^{\infty} \left[\varphi_n e^{-\mu_n t} \int_0^1 y_n(x) dx \right], \quad K(t,\tau) = \sum_{\substack{n=0 \\ (n \neq n_0)}}^{\infty} \left[f_n(\tau) e^{-\mu_n (t-\tau)} \int_0^1 y_n(x) dx \right]. \tag{2.6}$$

By using (2.2), under the assumptions (A_1) and (A_3), the term $F(t)$ and the kernel $K(t,\tau)$ are continuously differentiable functions in $[0,T]$ and $[0,T] \times [0,T]$, respectively. From (2.6), it is easy to show that

$$F(0) = \sum_{\substack{n=0 \\ (n \neq n_0)}}^{\infty} \left[\varphi_n \int_0^1 y_n(x) dx \right] = \int_0^1 \varphi(x) dx, \quad K(t,t) = \sum_{\substack{n=0 \\ (n \neq n_0)}}^{\infty} \left[f_n(\tau) \int_0^1 y_n(x) dx \right] = \int_0^1 f(x,t) dx.$$

Further, under the assumption (A_2), by differentiating Eq. (2.5) yields the following Volterra integral equation of the second kind:

$$K(t,t) r(t) + \int_0^t K_t(t,\tau) r(\tau) d\tau + F'(t) = E'(t). \tag{2.7}$$

Note that the function $K(t,t)$ is never equal to zero because of the assumption $\int_0^1 f(x,t) dx \neq 0, \forall t \in [0,T]$ in (A_3). In addition, the functions $F'(t), E'(t)$ and the kernel $K_t(t,\tau)$ are continuous functions in $[0,T]$ and $[0,T] \times [0,T]$, respectively. We therefore obtain a unique function $r(t)$, continuous in $[0,T]$, which, together with the solution of the problem (1.1)–(1.3), (1.5) given by the Fourier series (2.4), form the unique solution of the inverse problem (1.1)–(1.3), (1.5), (1.6). Theorem 1 has been proved. □

The solution of (2.7) is given by the series

$$r(t) = \sum_{n=0}^{\infty} (\mathbf{K}^n B)(t),$$

where $(\mathbf{K}B)(t) := \int_0^t Q(t,\tau) B(\tau) d\tau$ with $B(t) = \frac{E'(t) - F'(t)}{K(t,t)}$ and $Q(t,\tau) = -\frac{K_t(t,\tau)}{K(t,t)}$. It is easy to verify that

$$\left| (\mathbf{K}^n B)(t) \right| \leqslant \|B\|_{C[0,T]} \frac{\left(t \|Q\|_{C([0,T] \times [0,T])} \right)^n}{n!}, \quad t \in [0,T], \quad n = 0, 1, \ldots.$$

Thus, we obtain the estimate

$$\|r\|_{C[0,T]} \leqslant \|B\|_{C[0,T]} e^{T \|Q\|_{C([0,T] \times [0,T])}}. \tag{2.8}$$

We finally prove the continuous dependence on the data of the solution of the inverse problem (1.1)–(1.3), (1.5), (1.6).

Theorem 2 (*Continuous dependence upon the data*). *Let $\Im$ be the class of triples $\{f,\varphi,E\}$ which satisfy the assumptions $(A_1)-(A_3)$ of Theorem 1 and*

$$\|f\|_{C^{4,0}(\overline{D}_T)} \leqslant N_0, \quad \|\varphi\|_{C^4[0,1]} \leqslant N_1, \quad \|E\|_{C^1[0,T]} \leqslant N_2, \quad 0 < N_3 \leqslant \left|\int_0^1 f(x,t)dx\right|,$$

for some positive constants $N_i, i=\overline{0,3}$. Then the solution pair $(r(t),u(x,t))$ of the inverse problem (1.1)–(1.3), (1.5), (1.6) depends continuously upon the data in $\Im$.

Proof. Let $\{f,\varphi,E\}$ and $\{\tilde{f},\tilde{\varphi},\tilde{E}\}$ be two sets of data in $\Im$. Let $(r(t),u(x,t))$ and $(\tilde{r}(t),\tilde{u}(x,t))$ be the solutions of inverse problems (1.1)–(1.3), (1.5), (1.6) corresponding to these data.

According to (2.7) we have

$$r(t) = \int_0^t Q(t,\tau)r(\tau)d\tau + B(t), \quad \tilde{r}(t) = \int_0^t \widetilde{Q}(t,\tau)\tilde{r}(\tau)d\tau + \widetilde{B}(t), \tag{2.9}$$

with $B(t) = \dfrac{E'(t)-F'(t)}{K(t,t)}$, $Q(t,\tau) = -\dfrac{K_t(t,\tau)}{K(t,t)}$, $\widetilde{B}(t) = \dfrac{\widetilde{E}'(t)-\widetilde{F}'(t)}{\widetilde{K}(t,t)}$ and $\widetilde{Q}(t,\tau) = -\dfrac{\widetilde{K}_t(t,\tau)}{\widetilde{K}(t,t)}$.

Differentiating (2.6) we obtain

$$F'(t) = -\sum_{\substack{n=0\\(n\neq n_0)}}^{\infty}\left[\mu_n\varphi_n e^{-\mu_n t}\int_0^1 y_n(x)dx\right], \quad K_t(t,\tau) = -\sum_{\substack{n=0\\(n\neq n_0)}}^{\infty}\left[\mu_n f_n(\tau)e^{-\mu_n(t-\tau)}\int_0^1 y_n(x)dx\right].$$

According to (2.2) we have

$$|B(t)| \leqslant \frac{1}{|K(t,t)|}\left(|E'(t)|+|F'(t)|\right) \leqslant \frac{1}{N_3}\left(\|E\|_{C^1[0,T]} + c_4M\|\varphi\|_{C^4[0,1]}\right) \leqslant \frac{1}{N_3}(N_2 + c_4MN_1), \tag{2.10}$$

where M is the constant such that $M \geqslant |y_n(x)|$, $\forall n\in\mathbb{N}, \forall x\in[0,1]$.

Analogously, we can show that

$$\left|\widetilde{Q}(t,\tau)\right| \leqslant \frac{c_4M}{N_3}\max_{t\in[0,T]}\left\|\tilde{f}(\cdot,t)\right\|_{C^4[0,1]} \leqslant \frac{c_4MN_0}{N_3}. \tag{2.11}$$

Let us estimate the difference $r-\tilde{r}$. From (2.9) we obtain:

$$r(t)-\tilde{r}(t) = \int_0^t \widetilde{Q}(t,\tau)[r(\tau)-\tilde{r}(\tau)]d\tau + \int_0^t \left[Q(t,\tau)-\widetilde{Q}(t,\tau)\right]r(\tau)d\tau + B(t)-\widetilde{B}(t). \tag{2.12}$$

Denoting $R(t) = |r(t)-\tilde{r}(t)|$ and $H_1 = \left\|B-\widetilde{B}\right\|_{C[0,T]} + T\left\|Q-\widetilde{Q}\right\|_{C[0,T]\times C[0,T]}\|r\|_{C[0,T]}$, identity (2.12) implies that

$$R(t) \leqslant H_1 + \int_0^t \left|\widetilde{Q}(t,\tau)\right|R(\tau)d\tau.$$

Then, a Gronwall's-type inequality, see Theorem 16 of [26], implies that

$$R(t) \leqslant H_1 \exp\left(\int_0^t \sup_{\sigma\in[\tau,t]}\left|\widetilde{Q}(t,\tau)\right|d\tau\right), \quad t\in[0,T].$$

Using (2.11) we obtain

$$\|r-\tilde{r}\|_{C[0,T]} \leqslant M_0\left(\left\|B-\widetilde{B}\right\|_{C[0,T]} + T\left\|Q-\widetilde{Q}\right\|_{C[0,T]\times C[0,T]}\|r\|_{C[0,T]}\right), \tag{2.13}$$

where $M_0 = \exp\left(T\frac{c_4MN_0}{N_3}\right)$. Since $\|r\|_{C[0,T]} \leqslant \frac{M_0}{N_3}(N_2+c_4MN_1)$ (see (2.8) and (2.11)), it can be seen from (2.13) that r continuously depends upon B and Q.

By using the inequalities:

$$\left|F'(t)-\widetilde{F}'(t)\right| = \left|\sum_{\substack{n=0\\(n\neq n_0)}}^{\infty}\mu_n(\varphi_n-\tilde{\varphi}_n)e^{-\mu_n t}\int_0^1 y_n(x)dx\right| \leqslant c_4 M\|\varphi-\tilde{\varphi}_n\|_{C^4[0,1]},$$

$$\left|K_t(t,\tau)-\widetilde{K}_t(t,\tau)\right| = \left|\sum_{\substack{n=0\\(n\neq n_0)}}^{\infty}\mu_n\left(f_n(\tau)-\tilde{f}_n(\tau)\right)e^{-\mu_n(t-\tau)}\int_0^1 y_n(x)dx\right| \leqslant c_4 M\left\|f-\tilde{f}\right\|_{C^{4,0}(\overline{D}_T)},$$

$$\left|K(t,t)-\widetilde{K}(t,t)\right| = \left|\int_0^1\left(f(x,t)-\tilde{f}(x,t)\right)dx\right| \leqslant \left\|f-\tilde{f}\right\|_{C(\overline{D}_T)},$$

simple manipulations yield the estimates

$$\left|B(t)-\widetilde{B}(t)\right| \leqslant M_1\left\|E-\widetilde{E}\right\|_{C^1[0,T]} + M_2\|\varphi-\tilde{\varphi}\|_{C^4[0,1]} + M_3\left\|f-\tilde{f}\right\|_{C^{4,0}(\overline{D}_T)},$$

$$\left|Q(t,\tau)-\widetilde{Q}(t,\tau)\right| \leqslant M_4\left\|E-\widetilde{E}\right\|_{C^1[0,T]} + M_5\|\varphi-\tilde{\varphi}\|_{C^4[0,1]} + M_6\left\|f-\tilde{f}\right\|_{C^{4,0}(\overline{D}_T)},$$

where $M_k, k=\overline{1,6}$ are constants that are determined by c_4, M and $N_k, k=\overline{0,3}$. By using these inequalities, from (2.13) we obtain

$$\|r-\tilde{r}\|_{C[0,T]} \leqslant M_7\left(\left\|E-\widetilde{E}\right\|_{C^1[0,T]} + \|\varphi-\tilde{\varphi}\|_{C^4[0,1]} + \left\|f-\tilde{f}\right\|_{C^{4,0}(\overline{D}_T)}\right)$$

for some positive constant M_7. This means that r continuously depends upon the data.

Similarly, we can prove that u, which is given in (2.4), depends continuously upon the data. Theorem 2 has been proved. □

Theorems 1 and 2 in fact establish that the inverse problem under investigation given by Eqs. (1.1)–(1.3), (1.5), (1.6) is well-posed in appropriate spaces of regular functions. However, in practice the input data, especially the measured one, such as the energy (1.6), is non-smooth and hence, the solution of the inverse problem becomes unstable under unregularised inversion. The next section describes the discretisation of the inverse problem using the BEM, whilst Section 4 will discuss the regularization of the numerical solution.

3. Boundary element method (BEM)

In this section, we explain the numerical procedure for discretising the inverse problem (1.1)–(1.3), (1.5), (1.6) by using the BEM. First of all, let us introduce the fundamental solution G of the one-dimensional heat equation, as

$$G(x,t,y,\tau) = \frac{H(t-\tau)}{\sqrt{4\pi(t-\tau)}}\exp\left(-\frac{(x-y)^2}{4(t-\tau)}\right),$$

where H is the Heaviside step function. On multiplying the heat Eq. (1.1) by this fundamental solution and using the Green's identity, we obtain the following boundary integral equation, see e.g. [1]:

$$\eta(x)u(x,t) = \int_0^t\left[G(x,t,\xi,\tau)\frac{\partial u}{\partial n(\xi)}(\xi,\tau) - u(\xi,\tau)\frac{\partial G}{\partial n(\xi)}(x,t,\xi,\tau)\right]_{\xi\in\{0,1\}}d\tau + \int_0^1 G(x,t,y,0)u(y,0)\,dy + \int_0^1\int_0^T G(x,t,y,\tau)r(\tau)f(y,\tau)\,d\tau dy, \quad (x,t)\in[0,1]\times(0,T], \tag{3.1}$$

where $\eta(0)=\eta(1)=\frac{1}{2}, \eta(x)=1$ for $x\in(0,1)$, and $\underline{n}$ is the outward normal to the space boundary $\{0,1\}$. For discretising (3.1), we divide the boundaries $\{0\}\times[0,T]$ and $\{L\}\times[0,T]$ into N small time-intervals $[t_{j-1},t_j], j=\overline{1,N}$, with $t_j=\frac{jT}{N}, j=\overline{0,N}$, whilst the initial domain $[0,L]\times\{0\}$ is divided into N_0 small cells $[x_{k-1},x_k], k=\overline{1,N_0}$ with $x_k=\frac{k}{N_0}, k=\overline{0,N_0}$. Over each boundary element, the temperature u and the flux $\frac{\partial u}{\partial n}$ are assumed to be constant and take their values at the midpoint $\tilde{t}_j=\frac{t_{j-1}+t_j}{2}$, i.e.

$$u(1,t)=u(1,\tilde{t}_j)=:h_{1j}, \quad \frac{\partial u}{\partial n}(0,t)=\frac{\partial u}{\partial n}(0,\tilde{t}_j)=:q_{0j}, \quad \frac{\partial u}{\partial n}(1,t)=\frac{\partial u}{\partial n}(1,\tilde{t}_j)=:q_{1j},$$

for $t \in (t_{j-1}, t_j]$. Similarly, in each cell, the initial temperature $u(x,0)$ is assumed to be constant and takes its value at the mid-point $\tilde{x}_k = \frac{x_{k-1}+x_k}{2}$, i.e.

$$u(x,0) = \varphi(x) = \varphi(\tilde{x}_k) =: \varphi_k \quad \text{for} \quad x \in [x_{k-1}, x_k).$$

Applying the boundary condition (1.3), i.e. $u(0,t) = 0$, and using the constant BEM interpolations above, the boundary integral Eq. (3.1) becomes

$$\eta(x)u(x,t) = \sum_{j=1}^{N} [A_{0j}(x,t)q_{0j} + A_{1j}(x,t)q_{1j} - B_{1j}(x,t)h_{1j}] + \sum_{k=1}^{N_0} C_k(x,t)\varphi_k + s(x,t), \tag{3.2}$$

where the coefficients are given by

$$A_{\xi j}(x,t) = \int_{t_{j-1}}^{t_j} G(x,t,\xi,\tau)d\tau \quad \text{for} \quad \xi = \{0,1\}, \tag{3.3}$$

$$B_{1j}(x,t) = \int_{t_{j-1}}^{t_j} \frac{\partial G}{\partial n}(x,t,1,\tau)d\tau, \quad C_k(x,t) = \int_{x_{k-1}}^{x_k} G(x,t,y,0)dy, \tag{3.4}$$

for $j = \overline{1,N}, k = \overline{1,N_0}$, and the source double integral term is given by

$$s(x,t) = \int_0^1 \int_0^t G(x,t,y,\tau)r(\tau)f(y,\tau)d\tau dy. \tag{3.5}$$

This integral term can also be approximated using piecewise constant approximations for the functions $f(x,t)$ and $r(t)$ as

$$f(x,t) = f(x,\tilde{t}_j), \quad r(t) = r(\tilde{t}_j) =: r_j, \quad x \in (0,1), t \in (t_{j-1}, t_j], \quad j = \overline{1,N}.$$

Then we can approximate the double integral (3.5) as

$$s(x,t) = \int_0^t r(\tau) \int_0^1 G(x,t,y,\tau)f(y,\tau)\,dyd\tau = \sum_{j=1}^{N} D_j(x,t)r_j, \tag{3.6}$$

where

$$D_j(x,t) = \int_0^1 f(y,\tilde{t}_j)A_{yj}(x,t)\,dy, \quad j = \overline{1,N}. \tag{3.7}$$

The integrals in (3.3) and (3.4) can be evaluated analytically, [1], whereas the Simpson's rule is used as a numerical integration for calculating the integral (3.7). With the approximation (3.6), Eq. (3.2) becomes

$$\eta(x)u(x,t) = \sum_{j=1}^{N} [A_{0j}(x,t)q_{0j} + A_{1j}(x,t)q_{1j} - B_{1j}(x,t)h_{1j} + D_j(x,t)r_j] + \sum_{k=1}^{N_0} C_k(x,t)\varphi_k. \tag{3.8}$$

Applying (3.8) at the boundary nodes $(0,\tilde{t}_i)$ and $(1,\tilde{t}_i)$ for $i = \overline{1,N}$ gives the system of $2N$ equations

$$A_0\underline{q}_0 + A_1\underline{q}_1 - B_1\underline{h}_1 + D\underline{r} + C\underline{\varphi} = \underline{0}, \tag{3.9}$$

where

$$A_0 = \begin{bmatrix} A_{0j}(0,\tilde{t}_i) \\ A_{0j}(1,\tilde{t}_i) \end{bmatrix}_{2N\times N}, \quad A_1 = \begin{bmatrix} A_{1j}(0,\tilde{t}_i) \\ A_{1j}(1,\tilde{t}_i) \end{bmatrix}_{2N\times N}, \quad B_1 = \begin{bmatrix} B_{1j}(0,\tilde{t}_i) \\ B_{1j}(1,\tilde{t}_i) + \frac{1}{2}\delta_{ij} \end{bmatrix}_{2N\times N},$$

$$C = \begin{bmatrix} C_k(0,\tilde{t}_i) \\ C_k(1,\tilde{t}_i) \end{bmatrix}_{2N\times N_0}, \quad D = \begin{bmatrix} D_j(0,\tilde{t}_i) \\ D_j(1,\tilde{t}_i) \end{bmatrix}_{2N\times N},$$

$$\underline{q}_0 = [q_{0j}]_N, \quad \underline{q}_1 = [q_{1j}]_N, \quad \underline{h}_1 = [h_{1j}]_N, \quad \underline{\varphi} = [\varphi_k]_{N_0}, \quad \underline{r} = [r_j]_N,$$

where δ_{ij} is the Kronecker delta symbol.

In order to apply the boundary condition (1.5) we need to approximate the time-derivative $u_t(1,t)$ by using finite differences. For this, we use the $O(h^2)$ finite difference formulae

$$u_t(1,\tilde{t}_1) = \frac{u(1,\tilde{t}_2)/3 + u(1,\tilde{t}_1) - 4\varphi(1)/3}{h},$$

$$u_t(1,\tilde{t}_2) = \frac{5u(1,\tilde{t}_2)/3 - 3u(1,\tilde{t}_1) + 4\varphi(1)/3}{h},$$

$$u_t(1,\tilde{t}_i) = \frac{3u(1,\tilde{t}_i)/2 - 2u(1,\tilde{t}_{i-1}) + u(1,\tilde{t}_{i-2})/2}{h}, \quad i = \overline{3,N},$$

where $h = T/N$. Applying the expressions above into the boundary condition (1.5) yields the linear system of N equations as follows:

$$\begin{cases} \frac{a}{h}u(1,\tilde{t}_1) + \frac{a}{3h}u(1,\tilde{t}_2) + bu(1,\tilde{t}_1) = ar(\tilde{t}_1)f(1,\tilde{t}_1) + \frac{4a}{3h}\varphi(1) - du_x(1,\tilde{t}_1), \\ -\frac{3a}{h}u(1,\tilde{t}_1) + \frac{5a}{3h}u(1,\tilde{t}_2) + bu(1,\tilde{t}_1) = ar(\tilde{t}_2)f(1,\tilde{t}_2) - \frac{4a}{3h}\varphi(1) - du_x(1,\tilde{t}_2), \\ \frac{a}{2h}u(1,\tilde{t}_{i-2}) - \frac{2a}{h}u(1,\tilde{t}_{i-1}) + \frac{3a}{2h}u(1,\tilde{t}_i) + bu(1,\tilde{t}_i) = ar(\tilde{t}_i)f(1,\tilde{t}_i) - du_x(1,\tilde{t}_i), \quad i = \overline{3,N}. \end{cases}$$

This system can be rewritten as

$$S\underline{h}_1 = F\underline{r} + \underline{\tilde{\varphi}} - d\underline{q}_1, \tag{3.10}$$

where $F = \mathrm{diag}(f(1,\tilde{t}_1),\ldots,f(1,\tilde{t}_N))$, and

$$S = \begin{bmatrix} a/h+b & a/3h & 0 & . \\ -3a/h & 5a/3h+b & 0 & . \\ a/2h & -2a/h & 3a/2h+b & . \\ . & . & . & . \\ 0 & a/2h & -2a/h & 3a/2h+b \end{bmatrix}_{N\times N}, \quad \underline{\tilde{\varphi}} = \begin{bmatrix} 4a\varphi(1)/3h \\ -4a\varphi(1)/3h \\ 0 \\ . \\ 0 \end{bmatrix}_N.$$

Assuming $d \neq 0$, eliminating $\underline{q}_1$ between (3.9) and (3.10) results in

$$\begin{bmatrix} \underline{h}_1 \\ \underline{q}_0 \end{bmatrix} = \left[\left(\frac{1}{d}A_1 S + B_1 \right) \middle| -A_0 \right]^{-1} \left(\frac{1}{d}A_1 F\underline{r} + \frac{1}{d}A_1\underline{\tilde{\varphi}} + C\underline{\varphi} + D\underline{r} \right), \tag{3.11}$$

where the matrix which is inverted is a $2N \times 2N$ matrix formed with the $2N \times N$ block matrices $\left(\frac{1}{d}A_1S + B_1\right)$ and $-A_0$ separated by the vertical line.

Next, we collocate the over-determination condition (1.6), by using the midpoint numerical integration approximation, at the discrete time $\tilde{t}_i$ for $i = \overline{1,N}$, as

$$E_i := E(\tilde{t}_i) = \int_0^1 u(x,\tilde{t}_i)\,dx = \frac{1}{N_0}\sum_{k=1}^{N_0} u(\tilde{x}_k,\tilde{t}_i), \quad i = \overline{1,N}. \tag{3.12}$$

Using (3.2) at $(\tilde{x}_k,\tilde{t}_i)$, expression (3.12) can be rewritten as

$$\frac{1}{N_0}\sum_{k=1}^{N_0}\left[A_{0,k}^{(1)}\underline{q}_0 + A_{1,k}^{(1)}\underline{q}_1 - B_{1,k}^{(1)}\underline{h}_1 + C_k^{(1)}\underline{\varphi} + D_k^{(1)}\underline{r}\right] = \underline{E}, \tag{3.13}$$

where

$$A_{0,k}^{(1)} = \left[A_{0j}(\tilde{x}_k,\tilde{t}_i)\right]_{N\times N}, \quad A_{1,k}^{(1)} = \left[A_{1j}(\tilde{x}_k,\tilde{t}_i)\right]_{N\times N}, \quad B_{1,k}^{(1)} = \left[B_{1j}(\tilde{x}_k,\tilde{t}_i)\right]_{N\times N},$$
$$C_k^{(1)} = \left[C_l(\tilde{x}_k,\tilde{t}_i)\right]_{N\times N_0}, \quad D_k^{(1)} = \left[D_j(\tilde{x}_k,\tilde{t}_i)\right]_{N\times N}, \quad \underline{E} = [E_i]_N,$$

for $k,l = \overline{1,N_0}$ and $i,j = \overline{1,N}$. Finally, eliminating $\underline{q}_0, \underline{q}_1$ and $\underline{h}_1$ between (3.9)–(3.11), (3.13) the unknown discretised source $\underline{r}$ can be found by solving the $N \times N$ linear system of equations

$$X\underline{r} = \underline{y}, \tag{3.14}$$

where

$$X = \frac{1}{N_0}\sum_{k=1}^{N_0}\left\{ \left[\left(\frac{1}{d}A_{1,k}^{(1)}S + B_{1,k}^{(1)} \right) \middle| -A_{0,k}^{(1)} \right] \left[\left(\frac{1}{d}A_1 S + B_1 \right) \middle| -A_0 \right]^{-1} \left(\frac{1}{d}A_1 F + D \right) - \left(\frac{1}{d}A_{1,k}^{(1)}F + D_k^{(1)} \right) \right\},$$

$$\underline{y} = \frac{1}{N_0}\sum_{k=1}^{N_0}\left\{ C_k^{(1)}\underline{\varphi} + \frac{1}{d}A_{1,k}^{(1)}\underline{\tilde{\varphi}} - \left[\left(\frac{1}{d}A_{1,k}^{(1)}S + B_{1,k}^{(1)} \right) \middle| -A_{0,k}^{(1)} \right] \left[\left(\frac{1}{d}A_1 S + B_1 \right) \middle| -A_0 \right]^{-1} \left(C\underline{\varphi} + \frac{1}{d}A_1\underline{\tilde{\varphi}} \right) \right\} - \underline{E}.$$

Table 1
The RMSE for $u(1,t), u_x(0,t), u_x(1,t)$ and $E(t)$ obtained using the BEM for the direct problem with $N = N_0 \in \{20,40,80\}$, for Example 1.

$N = N_0$	RMSE			
	$u(1,t)$	$u_x(0,t)$	$u_x(1,t)$	$E(t)$
20	6.43E−3	2.79E−3	8.85E−3	2.65E−3
40	2.20E−3	9.68E−4	2.98E−3	9.07E−4
80	7.46E−4	3.32E−4	1.00E−3	3.08E−4

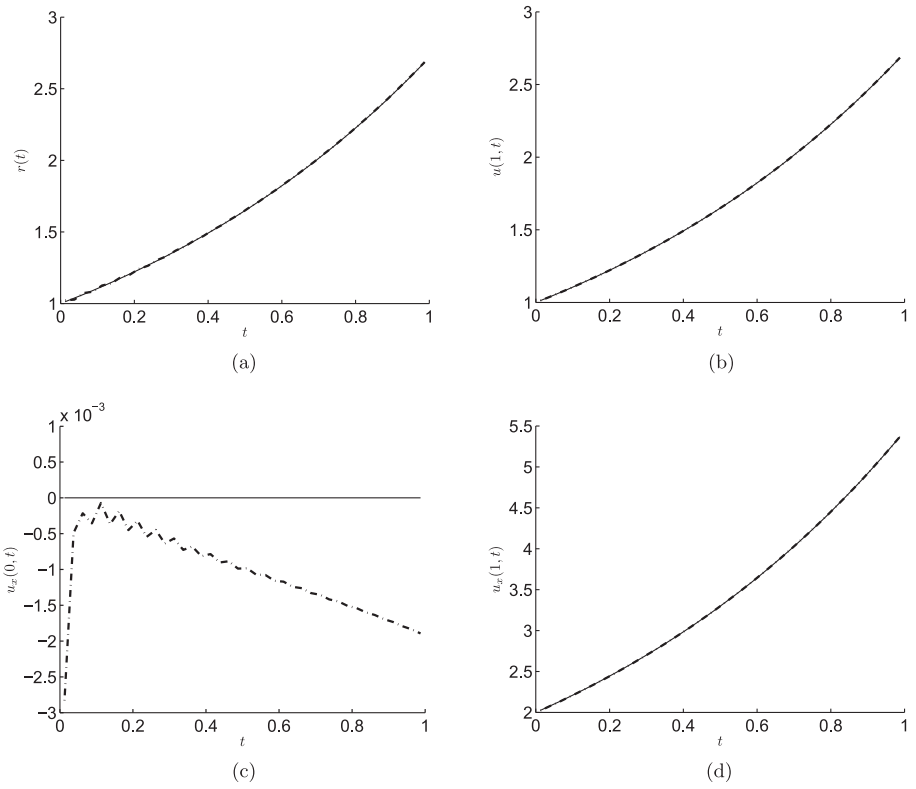

Fig. 1. The analytical (—) and numerical results (– · –) of (a) $r(t)$, (b) $u(1,t)$, (c) $u_x(0,t)$, and (d) $u_x(1,t)$ for exact data, for Example 1.

4. Numerical results and discussion

This section presents two benchmark test examples with smooth and non-smooth continuous source functions in order to test the accuracy of the BEM numerical procedure introduced earlier in Section 3. The following root mean square error (RMSE) is used to evaluate the accuracy of the numerical results:

$$\text{RMSE} = \sqrt{\frac{1}{N}\sum_{i=1}^{N}\left(Exact(\tilde{t}_i) - Approximate(\tilde{t}_i)\right)^2}. \tag{4.1}$$

4.1. Example 1

In this example, we consider the analytical solution given by

$$r(t) = e^t, \quad u(x,t) = x^2 e^t, \tag{4.2}$$

for the inverse problem (1.1)–(1.3), (1.5), (1.6) with the input data $T = 1, a = d = 1, b = -4, \varphi(x) = u(x,0) = x^2$ and $f(x,t) = x^2 - 2$. The direct problem (1.1)–(1.3), (1.5), when $r(t) = e^t$ is known, is considered first with $N = N_0 \in \{20, 40, 80\}$ obtained by (3.10), (3.11) and (3.13), and the RMSE results are shown in Table 1. From this table it can be concluded that the BEM numerical solution is convergent to the corresponding exact values

$$u(1,t) = e^t, \quad u_x(0,t) = 0, \quad u_x(1,t) = 2e^t, \quad E(t) = e^t/3, \quad t \in [0,1], \tag{4.3}$$

as the number of boundary elements increases.

Next, we consider the inverse problem (1.1)–(1.3), (1.5), (1.6) and we use the BEM with $N = N_0 = 40$ for solving the resulting system of Eqs. (3.14). Fig. 1 displays the analytical and numerical results of $r(t), u(1,t), u_x(0,t)$, and $u_x(1,t)$ and very good agreement can be observed.

In practice, the contamination of measured data by unplanned error is unavoidable. Thus we add noise to the input energy data $E(t)$ in (1.6) in order to test the stability of the solution. The perturbed input data $\underline{E}^{\epsilon}$ is defined as

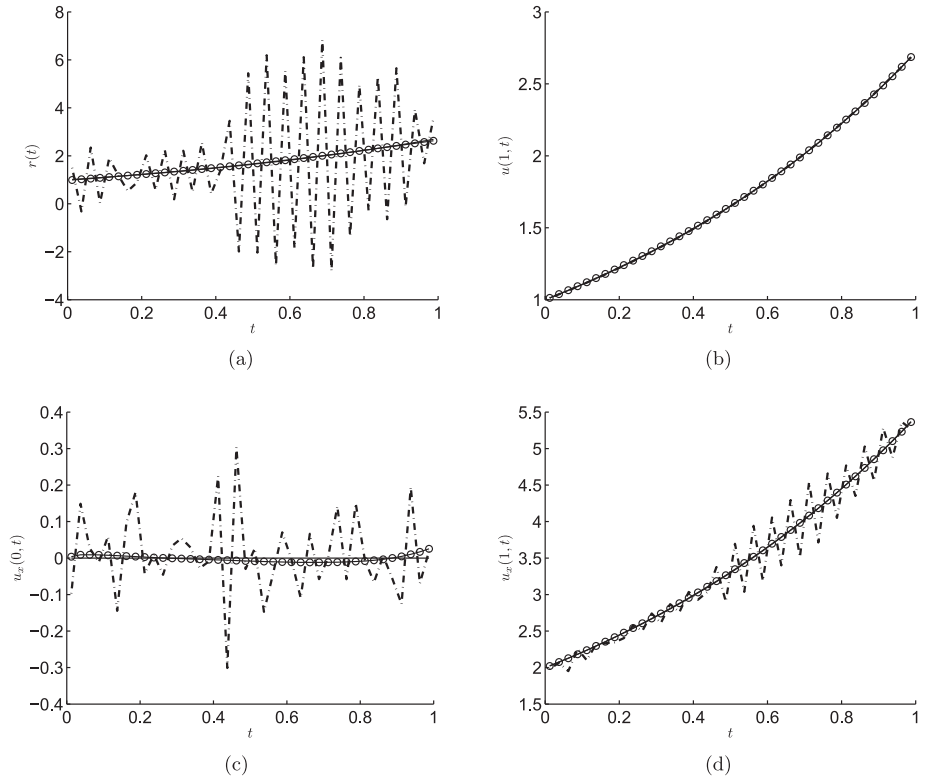

Fig. 2. The analytical (—) and numerical results of (a) $r(t)$, (b) $u(1,t)$, (c) $u_x(0,t)$, and (d) $u_x(1,t)$ obtained using the straightforward inversion $(- \cdot -)$ with no regularization, and the second-order Tikhonov regularization $(\circ\circ\circ)$ with the regularization parameter λ = 4.3E−6 suggested by the GCV method, for $p = 1\%$ noise, for Example 1.

$$\underline{E}^{\epsilon} = \underline{E} + \underline{\epsilon}, \tag{4.4}$$

where $\underline{\epsilon} = random('\text{Normal}', 0, \sigma, N, 1)$ is a set of N variables generated randomly by the MATLAB command from a normal distribution with the zero mean and standard deviation σ given by

$$\sigma = p \times \max_{t\in[0,T]} |E(t)| = \frac{ep}{3}, \tag{4.5}$$

where p is the percentage of noise. This perturbation means that the known right-hand side vector $\underline{y}$ is contaminated with noise, denoted as $\underline{y}^{\epsilon}$. Then, when noise is present, we have to solve the following system of linear equations instead of (3.14):

$$X\underline{r} = \underline{y}^{\epsilon}. \tag{4.6}$$

Fig. 2 illustrates the analytical and numerical results for $p = 1\%$ noise in the input data (4.4) obtained by the straightforward inversion of (4.6), i.e. $\underline{r} = X^{-1}\underline{y}^{\epsilon}$. From this figure it can be seen that the numerical solutions for $r(t), u_x(0,t)$ and $u_x(1,t)$ shown by the dash-dot line $(- \cdot -)$ are unstable. However, the result for $u(1,t)$ seems to remain stable and accurate.

To overcome this instability, we employ the second-order Tikhonov regularization method which gives

$$\underline{r}_{\lambda} = \left(X^{tr}X + \lambda R_2^{tr}R_2\right)^{-1} X^{tr}\underline{y}^{\epsilon}, \tag{4.7}$$

where $\lambda > 0$ is a regularization parameter to be prescribed and R_2 is a second-order differential regularization matrix, given by [27,28],

$$R_2^{tr}R_2 = \frac{1}{(T/N)^4}\begin{bmatrix} 1 & -2 & 1 & 0 & 0 & . & . & . \\ -2 & 5 & -4 & 1 & 0 & . & . & . \\ 1 & -4 & 6 & -4 & 1 & 0 & . & . \\ 0 & 1 & -4 & 6 & -4 & 1 & 0 & . \\ . & . & . & . & . & . & . & . \end{bmatrix}. \tag{4.8}$$

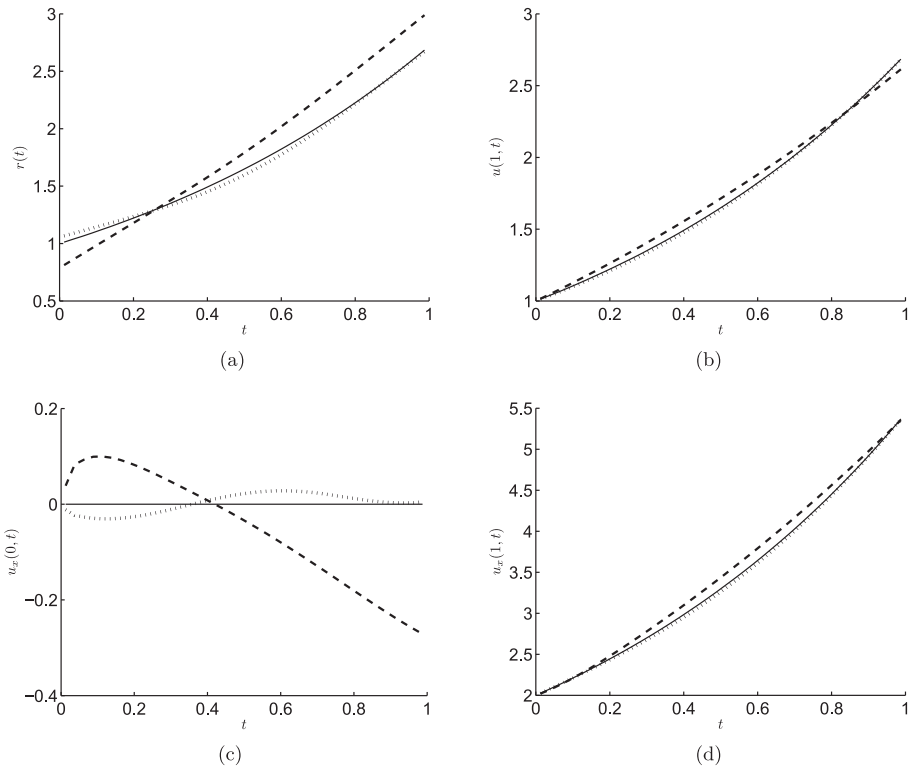

Fig. 3. The analytical (—) and numerical results of (a) $r(t)$, (b) $u(1,t)$, (c) $u_x(0,t)$, and (d) $u_x(1,t)$ obtained using the second-order Tikhonov regularization with the regularization parameter suggested by the GCV method, for $p = 3\%$ $(\cdots)$ and $p = 5\%$ $(---)$, for Example 1.

Table 2
The regularization parameters λ and the RMSE for $r(t), u(1,t), u_x(0,t)$ and $u_x(1,t)$, obtained using the BEM with $N = N_0 = 40$ combined with the second-order Tikhonov regularization for $p \in \{0,1,3,5\}\%$ noise, for Example 1.

p	λ	RMSE			
		$r(t)$	$u(1,t)$	$u_x(0,t)$	$u_x(1,t)$
0 (no noise)	0	4.16E−3	2.47E−4	1.20E−3	8.85E−4
1%	0	2.70	1.72E−2	1.12E−1	2.64E−1
1%	4.3E−6	1.73E−2	2.57E−3	8.92E−3	5.47E−3
3%	0	5.21	4.13E−2	3.51E−1	5.02E−1
3%	7.4E−6	3.32E−2	9.73E−3	1.97E−2	2.25E−2
5%	0	4.74	5.51E−2	4.64E−1	4.54E−1
5%	2.7E−5	1.95E−1	4.63E−2	1.29E−1	9.79E−2

As it happened previously with some of our investigations [3,4], we report that the second-order Tikhonov regularization has produced more accurate results than the zeroth- or first-order regularization and therefore, only the numerical results obtained using the former regularization are illustrated in this section.

A popular method for choosing the regularization parameter is the generalised cross-validation (GCV) criterion, which is based on minimising the following GCV function, [29]:

$$GCV(\lambda) = \frac{\|X(X^{tr}X + \lambda R_2^{tr}R_2)^{-1}X^{tr}\underline{y}^{\epsilon} - \underline{y}^{\epsilon}\|^2}{\left[\text{trace}(I - X(X^{tr}X + \lambda R_2^{tr}R_2)^{-1}X^{tr})\right]^2}. \tag{4.9}$$

For $p = 1\%$ noise, this minimization yields the minimum point of (4.9) occurring at λ = 4.3E−6. Then the numerical results obtained using (4.7) with this value of λ, illustrated by circles $(\circ\circ\circ)$ in Fig. 2, show that accurate and stable numerical solutions are achieved.

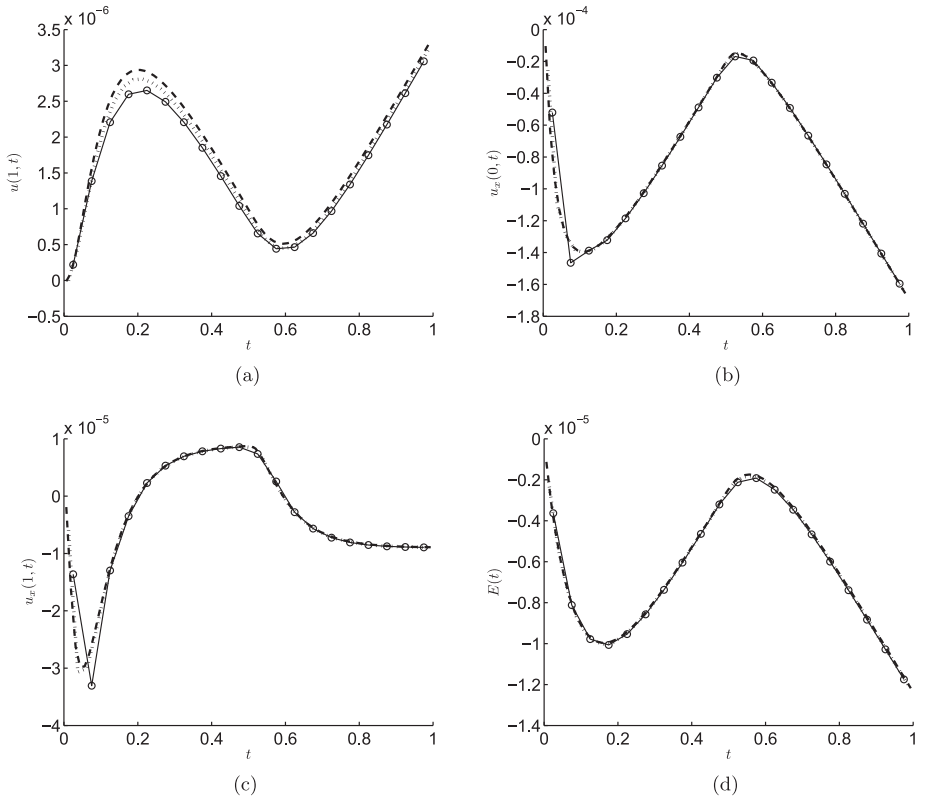

Fig. 4. The numerical results of (a) $u(1,t)$, (b) $u_x(0,t)$, (c) $u_x(1,t)$, and (d) $E(t)$ obtained by solving the direct problem with $N = N_0 \in \{20(\circ\circ\circ), 40(\cdots), 80(---)\}$, for Example 2.

Next, we increase to $p = 3\%$ and 5% the percentage of noise with which the data (4.4) is contaminated. Fig. 3 presents the analytical and numerical results obtained using the second-order Tikhonov regularization with the regularization parameter suggested by the GCV method, namely λ = 7.4E−6 for $p = 3\%$, and λ = 2.7E−5 for $p = 5\%$. From this figure one can observe that stable and accurate results for $r(t), u(1,t), u_x(0,t)$ and $u_x(1,t)$ with $p = 3\%$ noise are attained, whereas the numerical results for $p = 5\%$ noisy input are rather inaccurate, but they remain stable. For completeness, the RMSE errors (4.1) are displayed in Table 2.

4.2. Example 2

The previous example possessed an analytical solution being explicitly available; however the source function $f(x,t)$ chosen did not satisfy the condition in (A_3) of Theorem 1 that $f \in \Phi^4_{n_0}[0,1]$. Therefore, in this subsection we aim to construct an example for which the conditions of existence and uniqueness of solution of Theorem 1 are satisfied. We choose $T = 1, \varphi(x) = 0, a = d = 1$ and $b = 0$.

In the case $a = d = 1, b = 0$ the problem (1.8) has the eigenvalues $\mu_n = \nu_n^2$, where ν_n are the positive roots of the transcendental equation $\nu \sin(\nu) = \cos(\nu)$. The corresponding eigenfunctions are $y_n(x) = \sin(\nu_n x)$. The first eigenvalue is given by $\nu_0 = \sqrt{\mu_0} = 0.860333$. Then choosing $f(x,t) = x^3(1-x)^4(\beta_1 x + \beta_2)$ we can determine the constants β_1 and β_2 such that $f \in \Phi^4_0[0,1]$ (choosing $n_0 = 0$ for simplicity), as required by the condition (A_3) of Theorem 1. This imposes

$$0 = \int_0^1 f(x,t)\sin(\nu_0 x)\,dx = \int_0^1 x^3(1-x)^4(\beta_1 x + \beta_2)\sin(\nu_0 x)\,dx.$$

After some calculus, choosing $\beta_2 = -1$ it follows that $\beta_1 \approx 2.011$. With these values of β_1 and β_2 we also satisfy that $\int_0^1 f(x,t)\,dx = -0.00037$ is non-zero, as required by condition (A_3). We aim to retrieve a non-smooth source function given by

$$r(t) = \left|t - \frac{1}{2}\right|, \quad t \in [0,t]. \tag{4.10}$$

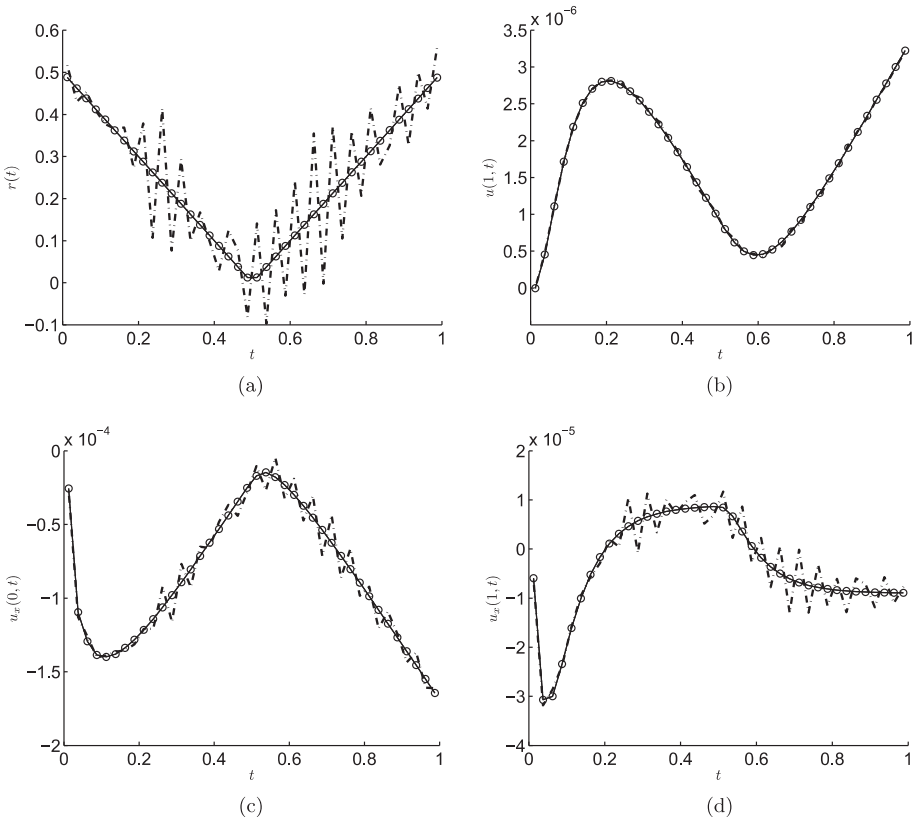

Fig. 5. The analytical solution (4.10) and the direct problem numerical solution from Fig. 4(a)–(c) (—) and numerical results of (a) $r(t)$, (b) $u(1,t)$, (c) $u_x(0,t)$, and (d) $u_x(1,t)$, with no regularization, for exact data ($\circ\circ\circ$) and noisy data $p = 1\%$ ($- \cdot -$), for Example 2.

In this case, the analytical solution of the direct problem for the temperature $u(x,t)$ is not available. Thus the energy $E(t)$ is not available either. In such a situation, we simulate the data (1.6) numerically by solving first the direct problem (1.1)–(1.3), (1.5) with r known and given by (4.10). The numerical solutions for $u(1,t), u_x(0,t), u_x(1,t)$ and $E(t)$ obtained using the BEM with $N = N_0 \in \{20, 40, 80\}$ are shown in Fig. 4. From this figure it can be seen that convergent numerical solutions are obtained.

To investigate the inverse problem (1.1)–(1.3), (1.5) and (1.6) we use the numerical results for $E(t)$ in Fig. 4(d) obtained using the BEM with $N = N_0 = 40$, as the input data (1.6). In order to avoid committing an inverse crime we keep $N = 40$, but we use a different N_0, say $N_0 = 30$, than 40 which was used in the direct problem simulation. Fig. 5 shows the numerical results obtained without regularization, i.e. $\lambda = 0$, for $p = 0$ (exact) and $p = 1\%$ (noisy) data. Remark that from Fig. 4(d), the standard deviation in (4.5) for Example 2 is given by $\sigma = 1.2 \times 10^{-5} p$. From Fig. 5 it can be seen that, for exact data, the straightforward inversion of (3.14) produces very accurate results. However, when noise is introduced into the measured data (4.4), the numerical retrievals of especially $r(t)$ and $u_x(1,t)$ become highly oscillatory unstable.

In order to retrieve the stability, as in Example 1, the second-order Tikhonov regularization with the GCV criterion are employed and the numerically obtained results are shown in Fig. 6. The numerical results from the direct problem presented in Fig. 4(a)–(c) are used to compare in Fig. 6(b)–(d) the numerical results for $u(1,t), u_x(0,t)$, and $u_x(1,t)$, respectively, of the inverse problem. Whereas the numerical solution for $r(t)$ of the inverse problem is compared with the analytical solution (4.10) in Fig. 6(a). From Fig. 6 it can be seen that stable and accurate numerical solutions are obtained. For completeness, the RMSE errors (4.1) and the GCV values for λ are displayed in Table 3.

If one would like to make a fair comparison between the accuracy of the numerical results obtained for Examples 1 and 2, the RMSE values presented in Tables 2 and 3 should be divided by the maximum absolute values of the corresponding quantities involved. For example, if we divide the columns of RMSE values for $r(t)$ in Tables 2 and 3 by e (maximum value of $r(t)$ in (4.2)) and 0.5 (maximum value of $r(t)$ in (4.10)), respectively, then the relative errors for $r(t)$ in Example 1 are actually lower than those in Example 2, as expected from the regularity of these solutions.

Finally, although not illustrated, it is reported that for both Examples 1 and 2 we have experienced with other values of λ close to the optimal ones but there was not much significant difference obtained in comparison with the numerical results of

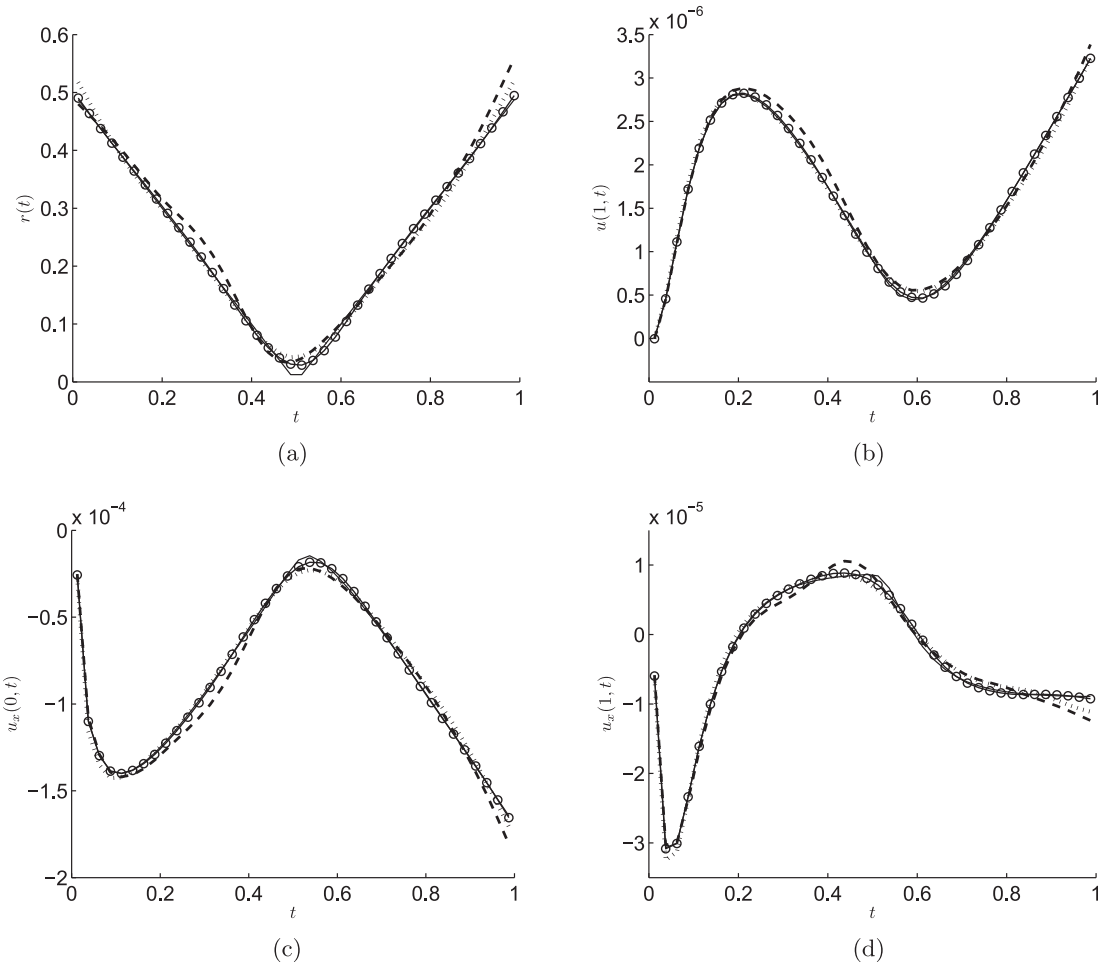

Fig. 6. The analytical solution (4.10) and the direct problem numerical solutions from Fig. 4(a)–(c) (—), and the numerical results of (a) $r(t)$, (b) $u(1,t)$, (c) $u_x(0,t)$, and (d) $u_x(1,t)$ obtained using the second-order Tikhonov regularization with the regularization parameters suggested by GCV method, for $p \in \{1(\circ\circ\circ), 3(\cdots), 5(---)\}\%$ noise, for Example 2.

Table 3
The regularization parameters λ and the RMSE for $r(t), u(1,t), u_x(0,t)$ and $u_x(1,t)$, obtained using the BEM with $N = 40$ and $N_0 = 30$ combined with the second-order Tikhonov regularization for $p \in \{0, 1, 3, 5\}\%$ noise, for Example 2.

p	λ	RMSE			
		$r(t)$	$u(1,t)$	$u_x(0,t)$	$u_x(1,t)$
0 (no noise)	0	2.90E−4	2.12E−10	2.94E−8	1.07E−8
1%	0	9.98E−2	2.71E−8	9.55E−6	3.55E−6
1%	3.2E−16	5.47E−3	1.62E−8	1.28E−6	4.12E−7
3%	0	3.63E−1	1.05E−7	3.39E−5	1.27E−5
3%	1.1E−15	1.37E−2	5.96E−8	3.56E−6	9.37E−7
5%	0	5.03E−1	1.70E−7	4.85E−5	1.80E−5
5%	9.0E−16	2.17E−2	9.88E−8	5.68E−6	1.21E−6

Figs. 2, 3 and 6. This confirms that the GCV criterion performs well in choosing a suitable regularization parameter for obtaining a stable and accurate numerical solution.

5. Conclusions

The inverse problem of finding the time-dependent heat source together with the temperature in the heat equation, under a non-classical dynamic boundary condition and an integral over-determination condition has been investigated.

Firstly, the existence, uniqueness, and continuous dependence upon the data of the classical solution of the inverse problem have been established. Next, a numerical method based on the BEM combined with the second-order Tikhonov regularization has been proposed together with the use of the GCV criterion for the selection of the regularization parameter. The retrieved numerical results were found to be accurate and stable on both smooth and non-smooth continuous examples.

As for the experimental validation of the proposed inverse mathematical model in terms of bias and inverting real noisy data we defer this challenging task to a possible future work. We only remark that unlike certain applications, e.g. some significant mismatch has been reported in [30–32] between experimental data of electromagnetic waves propagating in a non-attenuating medium and data produced by idealised computational simulations, in inverse heat conduction the mathematical models have been shown to perform much better in industrial applications with actual real measured data, [33].

Acknowledgements

A. Hazanee would like to acknowledge the financial support received from the Ministry of Science and Technology of Thailand, and Prince of Songkla University Thailand, for pursuing her PhD at the University of Leeds. The comments and suggestions made by the referees are gratefully acknowledged.

References

[1] A. Farcas, D. Lesnic, The boundary element method for the determination of a heat source dependent on one variable, J. Eng. Math. 54 (2006) 375–388.
[2] A. Hasanov, B. Pektas, Identification of an unknown time-dependent heat source term from overspecified Dirichlet boundary data by conjugate gradient method, Comput. Math. Appl. 65 (2013) 42–57.
[3] A. Hazanee, M.I. Ismailov, D. Lesnic, N.B. Kerimov, An inverse time-dependent source problem for the heat equation, Appl. Numer. Math. 69 (2013) 13–33.
[4] A. Hazanee, D. Lesnic, Determination of a time-dependent heat source from nonlocal boundary conditions, Eng. Anal. Boundary Elem. 37 (2013) 936–956.
[5] M.I. Ismailov, F. Kanca, D. Lesnic, Determination of a time-dependent heat source under nonlocal boundary and integral overdetermination conditions, Appl. Math. Comput. 218 (2011) 4138–4146.
[6] X. Xiong, Y. Yan, J. Wang, A direct numerical method for solving inverse heat source problems, J. Phys.: Conf. Ser. 290 (2011) 012017 (10 pages).
[7] L. Yang, M. Dehghan, J.N. Yu, G.W. Luo, Inverse problem of time-dependent heat sources numerical reconstruction, Math. Comput. Simul. 81 (2011) 1656–1672.
[8] N.B. Kerimov, M.I. Ismailov, Direct and inverse problems for the heat equation with a dynamic type boundary condition, IMA J. Appl. Math., submitted for publication, arXiv: 1306.4772.
[9] L. Bourgeois, N. Chaulet, H. Haddar, Stable reconstruction of generalized impedance boundary conditions, Inverse Prob. 27 (2011) 095002 (26 pages).
[10] L. Bourgeois, N. Chaulet, H. Haddar, On simultaneous identification of a scatterer and its generalized impedance boundary conditions, SIAM J. Sci. Comput. 34 (2012) 1824–1848.
[11] L. Bourgeois, H. Haddar, Identification of generalized impedance boundary conditions in inverse scattering problems, Inverse Prob. Imaging 4 (2010) 19–38.
[12] F. Cakoni, R. Kress, Integral equation method for the inverse obstacle problem with generalized impedance boundary condition, Inverse Prob. 29 (2013) 015005 (19 pages).
[13] R.E. Langer, A problem in diffusion or in the flow of heat for a solid in contact with a fluid, Tohoku Math. J. 35 (1932) 360–375.
[14] J.R. Cannon, The One-dimensional Heat Equation, Addison-Wesley Publishing Company, Menlo Park, California, 1984.
[15] D. Lesnic, L. Elliott, D.B. Ingham, R.J. Knipe, B. Clennell, The identification of hydraulic conductivities of composite rocks, in: G. Jones, Q. Fisher, R.J. Knipe (Ed.), Faulting, Fault Sealing and Fluid Flow in Hydrocarbon Reservoirs: Abstracts, Rock Deformation Research, Department of Earth Sciences, The University of Leeds, 1996, pp. 113–114.
[16] M. Slodicka, A parabolic inverse source problem with a dynamic boundary condition, Appl. Math. Comput., accepted for publication.
[17] N.I. Ionkin, Solution of a boundary-value problem in heat conduction with a non-classical boundary condition, Differ. Equ. 13 (1977) 294–304.
[18] E.C. Tichmarsh, Eigenfunction Expansions Associated with Second Order Differential Equations I, Oxford University Press, Oxford, 1962.
[19] J. Walter, Regular eigenvalue problems with eigenvalue parameter in the boundary conditions, Math. Z. 133 (1973) 301–312.
[20] P.A. Binding, P.J. Brown, K. Seddeghi, Sturm–Liouville problems with eigenparameter dependent boundary conditions, Proc. Edinburgh Math. Soc. 37 (1993) 57–72.
[21] C.T. Fulton, Two-point boundary value problems with eigenvalue parameter contained in the boundary conditions, Proc. R. Soc. Edinburgh: Sect. A Math. 77 (1977) 293–388.
[22] N.Y. Kapustin, E.I. Moiseev, Spectral problems with the spectral parameter in the boundary condition, Differ. Equ. 33 (1997) 115–119.
[23] N.B. Kerimov, T.I. Allakhverdiev, On a certain boundary value problem I, Differ. Equ. 29 (1993) 54–60.
[24] N.B. Kerimov, T.I. Allakhverdiev, On a certain boundary value problem II, Differ. Equ. 29 (1993) 952–960.
[25] N.B. Kerimov, V.S. Mirzoev, On the basis properties of one spectral problem with a spectral parameter in a boundary condition, Sib. Math. J. 44 (2003) 813–816.
[26] S.S. Dragomir, Some Gronwall Type Inequalities and Applications. RGMIA Monographs, Victoria University, Australia, 2002.
[27] A. Hazanee, D. Lesnic, Determination of a time-dependent coefficient in the bioheat equation, Int. J. Mech. Sci. 88 (2014) 259–266.
[28] S. Twomey, On the numerical solution of Fredholm integral equations of the first kind by the inversion of the linear system produced by quadrature, J. Assoc. Comput. Mach. 10 (1963) 97–101.
[29] L. Yan, C.L. Fu, F.L. Yang, The method of fundamental solutions for the inverse heat source problem, Eng. Anal. Boundary Elem. 32 (2008) 216–222.
[30] L. Beilina, N.T. Thanh, M.V. Klibanov, M.A. Fiddy, Reconstruction from blind experimental data for an inverse problem for a hyperbolic equation, Inverse Prob. 30 (2014) 025002 (24 pages).
[31] A.V. Kuzhuget, L. Beilina, M. Klibanov, A. Sullivan, L. Nguyen, M.A. Fiddy, Blind experimental data collected in the field and an approximately globally convergent inverse algorithm, Inverse Prob. 28 (2000) 095007 (33 pages).
[32] N.T. Thanh, L. Beilina, M. Klibanov, M.A. Fiddy, Reconstruction of the refractive index from experimental backscattering data using a globally convergent inverse method, SIAM J. Sci. Comput. 36 (2014) B273–B293.
[33] L. Elden, F. Berntsson, T. Reginska, Wavelet and Fourier methods for solving the sideways heat equation, SIAM J. Sci. Comput. 21 (2000) 2187–2205.